

# Bose-Einstein condensation and liquid-gas phase transition in $\alpha$ -matter

L. M. Satarov,<sup>1,2</sup> M. I. Gorenstein,<sup>1,3</sup> A. Motornenko,<sup>1,4,5</sup>

V. Vovchenko,<sup>1,6,4</sup> I. N. Mishustin,<sup>1,2</sup> and H. Stoecker<sup>1,6,7</sup>

<sup>1</sup> *Frankfurt Institute for Advanced Studies,  
D-60438 Frankfurt am Main, Germany*

<sup>2</sup> *National Research Center "Kurchatov Institute" 123182 Moscow, Russia*

<sup>3</sup> *Bogolyubov Institute for Theoretical Physics, 03680 Kiev, Ukraine*

<sup>4</sup> *Department of Physics, Taras Shevchenko  
National University of Kiev, 03022 Kiev, Ukraine*

<sup>5</sup> *Department of Physics, University of Oslo, 0313 Oslo, Norway*

<sup>6</sup> *Institut für Theoretische Physik, Goethe Universität Frankfurt,  
D-60438 Frankfurt am Main, Germany*

<sup>7</sup> *GSI Helmholtzzentrum für Schwerionenforschung GmbH, D-64291 Darmstadt, Germany*

## Abstract

Systems of Bose particles with both repulsive and attractive interactions are studied using the Skyrme-like mean-field model. The phase diagram of such systems exhibits two special lines in the chemical potential–temperature plane: one line which represents the first-order liquid-gas phase transition with the critical end point, and another line which represents the onset of Bose-Einstein condensation. The calculations are made for strongly-interacting matter composed of  $\alpha$  particles. The phase diagram of this matter is qualitatively similar to that observed for the atomic  $^4\text{He}$  liquid. The sensitivity of the results to the model parameters is studied. For weak interaction coupling the critical point is located at the Bose-condensation line.

## I. INTRODUCTION

Bose-Einstein condensation (BEC) in non-interacting boson systems was theoretically predicted a long time ago [1, 2]. However, only in 1995 two groups succeeded to create the necessary experimental conditions of very cold and dilute atomic Bose gases by using novel developments in cooling and trapping techniques [3, 4]. Currently, investigation of quantum phenomena in cold systems of interacting bosons is a subject of active theoretical [5, 6] and experimental [7] studies.

The first-order liquid-gas phase transition (LGPT), on the other hand, is a well-known phenomenon that occurs in systems of interacting atoms or molecules [8, 9] as well as in nuclear matter [10, 11]. The LGPT is a consequence of inter-particle interactions containing both attractive and repulsive forces. The observed phase diagram of atomic  $^4\text{He}$  [12] contains simultaneously the regions of the LGPT and the BEC. Note that the superfluidity phenomenon in Bose liquids appears only for nonzero interactions of particles [13].

In the present paper we study the phase diagram of matter composed of  $\alpha$  particles with strong (nuclear) interactions. It is commonly accepted that  $\alpha$  particles and  $\alpha$ -cluster correlations are important in atomic nuclei, in intermediate-energy heavy-ion collisions, and in astrophysical environments. This is due to the large binding energy of  $\alpha$  particles as compared to other light clusters like  $d, t, ^3\text{He}$ . Theoretical and experimental studies of nuclear systems with  $\alpha$  clusters have already a long history. The energy density of cold homogeneous  $\alpha$ -matter was estimated by using realistic  $\alpha\alpha$  potentials in Refs. [14, 15]. It was shown that such  $\alpha$ -matter is energetically favorable at low baryon densities (i.e., it has a larger binding energy per baryon) as compared to uniform nucleon matter.

It is believed that  $\alpha$  clusters exist either at periphery of heavy nuclei or in low-density excited states of light nuclei like  $^{12}\text{C}$ ,  $^{16}\text{O}$ ,  $^{20}\text{Ne}$ , etc. [16–18]. Especially interesting is the second excited (Hoyle) state of  $^{12}\text{C}$  which plays a key role in stellar nucleosynthesis. As argued in Ref. [19] the Hoyle state can be regarded as the Bose-condensed coherent state of  $3\alpha$  particles. Enhanced yields of  $\alpha$  particles have been observed in multifragmentation reactions in heavy-ion collisions [20–22]. Considerable abundances of  $\alpha$  clusters are expected in the outer regions of compact stars, in neutron star mergers, and in supernova matter [23, 24].

Different theoretical methods were used to study the equation of state of nuclear matter

with nucleons and light nuclei at various temperatures and baryon densities. In particular, phenomenological liquid-drop models were applied in Refs. [25, 26]. The chemically equilibrated  $N + \alpha$  mixture has been studied [27] by using the virial expansion, and the relativistic mean-field approach was used in Refs. [23, 28]. Lattice calculations for  $\alpha$ -matter were presented in Ref. [29].

In the present study we calculate the phase diagram of pure  $\alpha$ -matter using the mean-field Skyrme-like interaction. In contrast to other authors, we study simultaneously both, the LGPT and BEC. The article is organized as follows. In Sec. II the model is formulated. The phase diagrams for different pairs of thermodynamical variables are presented and discussed in Sec. III. The sensitivity of the results to the model parameters is also considered in this section. Conclusions and outlook are given in Sec. IV.

## II. BOSONIC SYSTEM WITH SKYRME INTERACTION

Let us consider a system of interacting bosons with mass  $m$  and degeneracy factor  $g$ . The grand canonical pressure  $p(T, \mu)$  is a function of temperature  $T$  and chemical potential  $\mu$  and plays the role of the thermodynamical potential. The particle number density  $n(T, \mu)$ , the entropy density  $s(T, \mu)$ , and the energy density  $\varepsilon(T, \mu)$  are calculated from  $p(T, \mu)$  as

$$n = \left( \frac{\partial p}{\partial \mu} \right)_T, \quad s = \left( \frac{\partial p}{\partial T} \right)_\mu, \quad \varepsilon = Ts + \mu n - p \quad (1)$$

in the thermodynamic limit, where the system volume goes to infinity.

In the present paper, both attractive and repulsive interactions are described in the mean-field approximation, by introducing the potential  $U(n)$  which depends on the particle density  $n$ , but does not depend on  $T$  [30, 31]. This is achieved by shifting the chemical potential with respect to the ideal gas value,

$$\mu^* = \mu - U(n). \quad (2)$$

Thermodynamical consistency requires then an additional (field) term in the pressure  $p_f$  (for more details see Refs. [32, 33]):

$$p(T, \mu) = p_{\text{id}}(T, \mu^*) + p_f(n), \quad p_f(n) = nU(n) - \int_0^n dn' U(n'). \quad (3)$$

In general, particle number density can be written as

$$n(T, \mu) = n_{\text{id}}(T, \mu^*) + n_{\text{bc}}. \quad (4)$$

The second term denotes the density of the Bose condensate which consists of zero-momentum particles. An explicit procedure of calculating  $n_{\text{bc}}$  is given below.

The ideal Bose gas pressure and particle number density in Eqs. (3) and (4) are, respectively, ( $\hbar = c = 1$ )

$$p_{\text{id}}(T, \mu^*) = \frac{g}{6\pi^2} \int_0^\infty dk \frac{k^4}{\sqrt{k^2 + m^2}} \left[ \exp\left(\frac{\sqrt{k^2 + m^2} - \mu^*}{T}\right) - 1 \right]^{-1}, \quad (5)$$

$$n_{\text{id}}(T, \mu^*) = \frac{g}{2\pi^2} \int_0^\infty dk k^2 \left[ \exp\left(\frac{\sqrt{k^2 + m^2} - \mu^*}{T}\right) - 1 \right]^{-1}. \quad (6)$$

Note that Eqs. (5) and (6) are only valid for  $\mu^* \leq m$ . A macroscopic fraction of zero momentum particles is accumulated at  $\mu^* = m$  forming a Bose condensate with nonzero density  $n_{\text{bc}}$ .

In the spirit of the Skyrme model [34, 35] we parameterize the mean-field potential as

$$U(n) = -an \left[ 2 - \frac{\gamma + 2}{\gamma + 1} \left( \frac{n}{n_0} \right)^\gamma \right]. \quad (7)$$

Here  $a$ ,  $n_0$ , and  $\gamma$  are the positive model parameters. Substituting (7) into Eq. (3) yields

$$p_f(n) = -an^2 \left[ 1 - \left( \frac{n}{n_0} \right)^\gamma \right]. \quad (8)$$

Note that the first terms on the right hand sides of Eqs. (7) and (8) correspond to attractive interactions between particles. Their form is identical to the van der Waals model [8, 9]. The second terms in these equations describe the repulsive interactions at short inter-particle distances. Note that  $p_f(n_0) = 0$ , and the point  $T = 0$  and  $n = n_0$  defines the ground state of the system. This is the case for all values  $a > 0$ . It is a consequence of a special form (7) of the potential  $U(n)$ , where both attractive and repulsive terms are proportional to the coupling constant  $a$ .

Similar parameterizations of the nucleon mean-field interaction are often used to describe properties of cold nucleon matter. Reasonable values of the nuclear matter compressibility are obtained for  $1/6 \leq \gamma \leq 1/3$  [34]. We use the same interval of  $\gamma$  values in our calculations.

The BEC in the ideal Bose gas (i.e., at  $a = 0$ ) occurs at  $\mu^* = \mu = m$ . At  $a > 0$ , this condition is replaced by  $\mu^* = \mu - U(n) = m$ , which can be written as

$$\mu = m + U(n_{\text{id}}(T, m) + n_{\text{bc}}). \quad (9)$$

Equation (9) with  $n_{\text{bc}} = 0$  defines the line  $T = T_{\text{BEC}}(\mu)$  in the  $(\mu, T)$  plane which corresponds to the onset of the BEC. Below this line, Eq. (9) gives nonzero values of  $n_{\text{bc}}$  as a function of  $T$  and  $\mu$ .

Substituting  $\mu^* = m$  into Eq. (6), one obtains in the lowest order in  $T/m$

$$n_{\text{id}}(T, m) = g \left( \frac{mT}{2\pi} \right)^{3/2} \left[ \zeta(3/2) + \frac{15}{8} \frac{T}{m} \zeta(5/2) + \dots \right]. \quad (10)$$

Here  $\zeta(x) = \sum_{k=1}^{\infty} k^{-x}$  is the Riemann zeta-function,  $\zeta(3/2) \cong 2.612$  and  $\zeta(5/2) \cong 1.341$ . The first term on the right hand side of Eq. (10) is the well-known nonrelativistic result [8, 9], and the second term gives a relativistic correction. The line  $T = T_{\text{BEC}}(n)$  obtained from Eq. (10) with  $n_{\text{id}} = n$  describes the onset of the BEC in the  $(n, T)$  plane. This line is ‘universal’, i.e., it does not depend on the interaction strength, and thus coincides with that for the ideal Bose gas. Neglecting relativistic corrections in Eq. (10) yields

$$T_{\text{BEC}}(n) \simeq \frac{2\pi}{m} \left[ \frac{n}{\zeta(3/2)g} \right]^{2/3}. \quad (11)$$

Equation (11) remains valid for the whole class of mean-field models with any potential  $U(n)$  which does not depend on  $T$ .

All thermodynamic functions can be calculated by using the above equations. The main feature of the LGPT is the appearance of the mixed phase which consists of ‘gas’ ( $n = n_g$ ) and ‘liquid’ ( $n = n_l$ ) domains with densities  $n_g < n_l$  at fixed  $T$ . The mixed-phase boundaries (the so-called binodals) in the  $(n, T)$  plane are found from the Gibbs conditions of the phase equilibrium:

$$p(n_g, T) = p(n_l, T), \quad \mu(n_g, T) = \mu(n_l, T). \quad (12)$$

The critical point (CP),  $T = T_c$  and  $n = n_c$ , is the ‘end point’ of the LGPT line in the  $(\mu, T)$  plane. At this point, both, the first and the second density derivative of the pressure vanish,  $(\partial p / \partial n)_T = 0$  and  $(\partial^2 p / \partial n^2)_T = 0$  [8, 9].

Fluctuations of thermodynamic variables play an important role in the physics of phase transitions. Especially interesting for nuclear systems are fluctuations of the particle number

in a fixed volume. They are characterized by the scaled variance of particle number fluctuations,  $\omega = \langle(\Delta N)^2\rangle/\langle N\rangle$ . Using Eqs. (6) and (2), one obtains the following expression (see also Refs. [36, 37]):

$$\omega = T \left( \frac{\partial p}{\partial n} \right)_T^{-1} = \frac{T}{n} \left( \frac{\partial n}{\partial \mu} \right)_T = \omega_{\text{id}}(T, \mu^*) \left[ 1 + \frac{n U'(n) \omega_{\text{id}}(T, \mu^*)}{T} \right]^{-1}, \quad (13)$$

where  $\omega_{\text{id}} = (T/n_{\text{id}}) (\partial n_{\text{id}}/\partial \mu^*)_T$  is the scaled variance for the ideal Bose gas.

The conditions  $(\partial p/\partial n)_T = 0$  and  $\omega = \infty$  are fulfilled at the CP (see e.g., Refs. [8, 9]). This in turn implies that the relation  $nU' = -T/\omega_{\text{id}}$  holds at the CP. Note that Eq. (13) is not applicable for unstable states where  $(\partial p/\partial n)_T < 0$ .

In addition to the CP, the BEC is another potential source of anomalous particle number fluctuations: indeed, in the ideal Bose gas one has  $\omega_{\text{id}} \rightarrow \infty$  at the onset of the BEC [38], i.e., at  $\mu = \mu^* \rightarrow m$ . This is, however, not the case in the model considered here. Using Eq. (13) one obtains the finite values  $\omega = T/[nU'(n)]$  in the limit  $\mu^* \rightarrow m$ .

### III. PHASE DIAGRAM OF $\alpha$ -MATTER

In this section we present results for the matter composed of  $\alpha$ -particles ( $g = 1$ ,  $m \simeq 3727$  MeV). Unless stated otherwise, the calculations are done for the following set of the model parameters:  $a = 3$  GeV fm<sup>3</sup>,  $\gamma = 1/6$ ,  $n_0 = 0.05$  fm<sup>-3</sup>. The corresponding values for  $T_c$  and  $n_c$  are presented in Table I.

In the Boltzmann approximation,  $p_{\text{id}} = nT$  and  $\omega_{\text{id}} = 1$ , one gets the following simple relations for critical temperature and density:

$$T_c = - n_c U'(n_c) = n_c^2 U''(n_c). \quad (14)$$

The second equality follows from  $(\partial^2 p/\partial n^2)_T = 0$ . Equations (7) and (14) lead to

$$T_c = \frac{2\gamma}{\gamma + 1} a n_c, \quad n_c = n_0 \left[ \frac{2}{(\gamma + 1)(\gamma + 2)} \right]^{1/\gamma}. \quad (15)$$

One can see that  $T_c$  is proportional to  $a$ , and  $n_c$  is independent of  $a$ . For a given set of model parameters Eq. (15) one obtains  $T_c \simeq 10.5$  MeV and  $n_c \simeq 0.012$  fm<sup>-3</sup>, in a good agreement with the values in Table I. However, as will be shown below, the Boltzmann approximation breaks down for  $a \rightarrow 0$ .

In Figs. 1 (a) and (b) the first-order LGPT is shown by solid lines and the BEC by dashed lines in the  $(\mu, T)$  and  $(T, p)$  planes, respectively. The LGPT line corresponds to the mixed phase states. At  $T < T_c$ , there is a discontinuity between the particle densities ( $n_l > n_g$ ) on the two sides of this line. The entropy and energy density jump across the LGPT line, whereas the pressure is continuous.

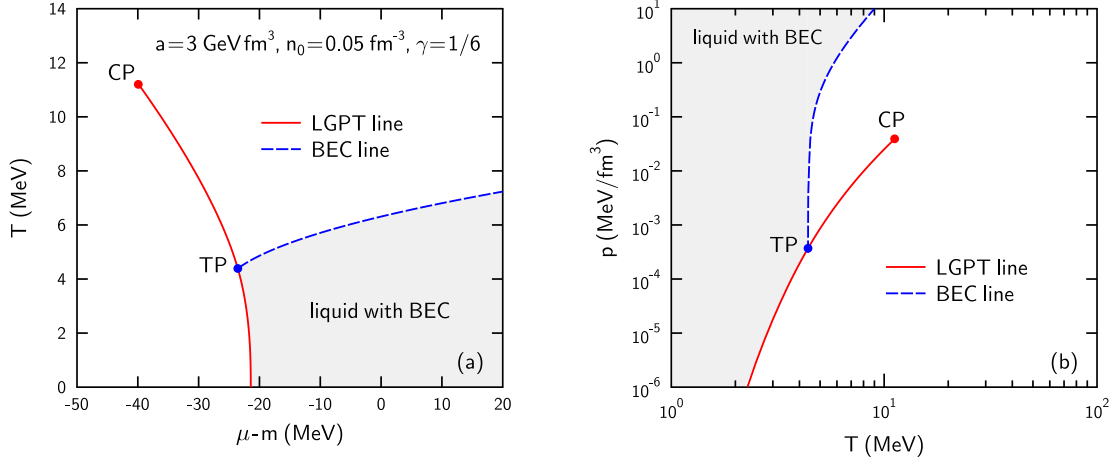


FIG. 1: Phase diagram of  $\alpha$ -matter in  $(\mu, T)$  (a) and  $(T, p)$  (b) planes. Solid lines correspond to the LGPT and dashed lines to the onset of the BEC. The CP and TP are marked by dots.

The shaded regions in Fig. 1 correspond to states with nonzero condensate density  $n_{bc}$ . The CP lies above the BEC boundary. Thus, the LGPT and the BEC lines intersect at some point which we call for brevity as the triple point (TP). Characteristics of the CP and TP are given in Table I. The phase diagram of the  $\alpha$ -matter in the  $(T, p)$  plane shown in Fig. 1 (b) is qualitatively similar to that observed [12] for atomic  $^4\text{He}$ -matter<sup>1</sup>.

TABLE I: Characteristics of the CP and TP for  $\alpha$ -matter with Skyrme interaction (here  $a = 3 \text{ GeV fm}^3$ ,  $n_0 = 0.05 \text{ fm}^{-3}$ ,  $\gamma = 1/6$  are used).

	$T$ (MeV)	$n$ ( $\text{fm}^{-3}$ )	$p$ ( $\text{MeV}/\text{fm}^3$ )	$\mu - m$ (MeV)
CP	11.2	0.013	$3.92 \cdot 10^{-2}$	-39.9
TP	4.39	0.045	$3.08 \cdot 10^{-4}$	-23.6

<sup>1</sup> In that case the BEC region and the TP are usually called as the HeII phase and the  $\lambda$  point, respectively.

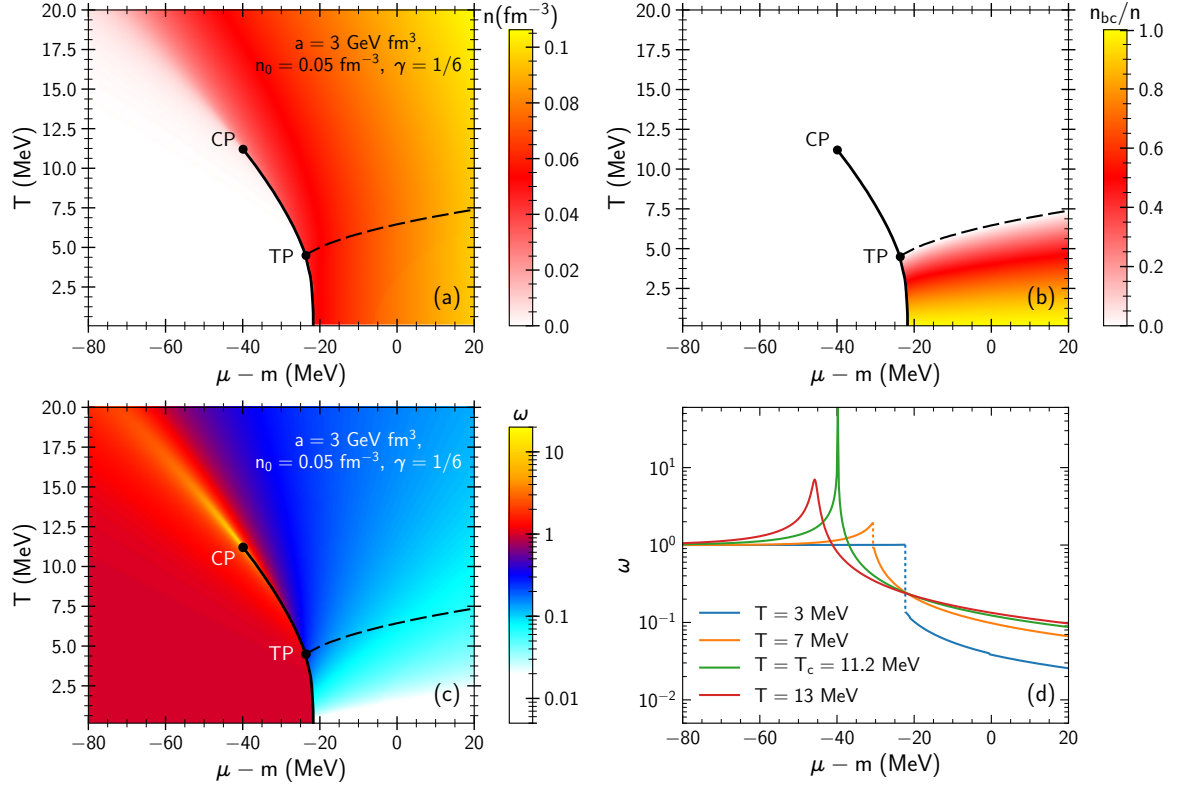


FIG. 2: Contour plots of the total density  $n$  (a), the relative fraction of Bose-condensed particles  $n_{bc}/n$  (b), and the scaled variance  $\omega$  (c) calculated for  $\alpha$ -matter. Panel (d) shows isotherms of  $\omega$  for several values of  $T$ . The solid and dashed curves show the LGPT and BEC lines, respectively. The CP and TP are marked by dots.

Figures 2 (a) and (b) show, respectively, the contour plots of the density  $n$  and the ratio  $n_{bc}/n$  in the  $(\mu, T)$  plane. The LGPT is shown in Fig. 2 by a solid line. The discontinuity of the density  $n$  across this line is clearly visible in Fig. 2 (a). At  $T < T_{TP}$  the gas of  $\alpha$ -particles with  $n = n_g$  and  $n_{bc} = 0$  coexists with the liquid domains with  $n = n_l > n_g$  and nonzero  $n_{bc}$ . One can see that above the CP very rapid, although continuous, changes of density occur in a narrow region of the  $(\mu, T)$  plane. This is a manifestation of the so-called crossover phenomenon.

The onset of the BEC is shown in Fig. 2 by dashed lines. The Bose condensate exists only in the liquid phase below this line. Figure 2 (b) shows that the normalized density of the Bose condensate,  $n_{bc}/n$ , starts from zero on the dashed line and goes to its maximum value,  $n_{bc}/n = 1$ , for  $T \rightarrow 0$ .

The contour plot of  $\omega$  in the  $(\mu, T)$  plane is shown in Fig. 2 (c). We have checked

that  $\omega$  is positive and finite for all states except the CP where it goes to infinity. Such a behavior strongly deviates from the ideal Bose gas where  $\omega = \omega_{\text{id}} = \infty$  for all states with  $\mu = \mu^* = m$  [38]. A more detailed information is shown in Fig. 2 (d) which represents  $\omega$  isotherms for temperatures above, below and near  $T_c$ . One can see jumps of  $\omega$  across the LGPT line.

Figures 3 (a) and (c) show the phase diagram of the  $\alpha$ -matter in the  $(n, T)$  and  $(n, p)$  planes, respectively, for the same model parameters as in Fig. 1. The ground state (GS),  $T = 0$  and  $n = n_0$ , has the minimum energy per particle and zero pressure. Thin dashed curves represent parts of the BEC lines inside the mixed phase region.

The calculation shows that the Boltzmann approximation (15) is rather accurate at large values of  $a$ , but it breaks down at small  $a$  as shown in Fig. 4. The CP can be found as the intersection of spinodal lines which go through the local minima and maxima of pressure isotherms. Let us consider points of the right-hand side (RHS) spinodal in the  $(n, T)$  plane as a function of temperature. At small  $T$ , the states on this spinodal can be found analytically by solving the equation  $(\partial p / \partial n)_T = 0$ . Below the BEC line  $\mu^* = m$ , the first term in (3) does not contribute to  $(\partial p / \partial n)_T$ , and, therefore, the above equation is equivalent to the condition  $p'_f(n) = 0$ . From Eq. (8) we conclude that the RHS spinodal at  $T \leq T_{\text{BEC}}(n^*)$  corresponds to a fixed density  $n = n^*$ :

$$n^* = n_0 \left( \frac{2}{2 + \gamma} \right)^{1/\gamma}, \quad (16)$$

On the other hand, the left-hand side spinodal lies above the BEC line. This proves that  $T_c \geq T_{\text{BEC}}(n^*)$  for all values of  $a$ .

At large enough values of the coupling constant  $a$  the CP position is above the BEC line, i.e., the states at the RHS spinodal move further to the left ( $n < n^*$ ) and upwards ( $T > T_{\text{BEC}}(n^*)$ ) in the  $(n, T)$  plane. In particular, this occurs, for the model parameters given in Table I. However, at small values of  $a$  the situation is changed. One can calculate analytically the behavior of  $(\partial p_{\text{id}} / \partial n)_T$  at  $(m - \mu^*) \rightarrow 0$  [38], i.e., in the vicinity of the BEC line. The calculation shows that if the condition

$$a \leq a_s = \frac{\zeta^2(3/2)}{4\pi} \frac{T_{\text{BEC}}(n^*)}{\gamma n^*} \quad (17)$$

holds, then the equation  $(\partial p / \partial n)_T = 0$  has no solutions at  $T > T_{\text{BEC}}(n^*)$ . In this case

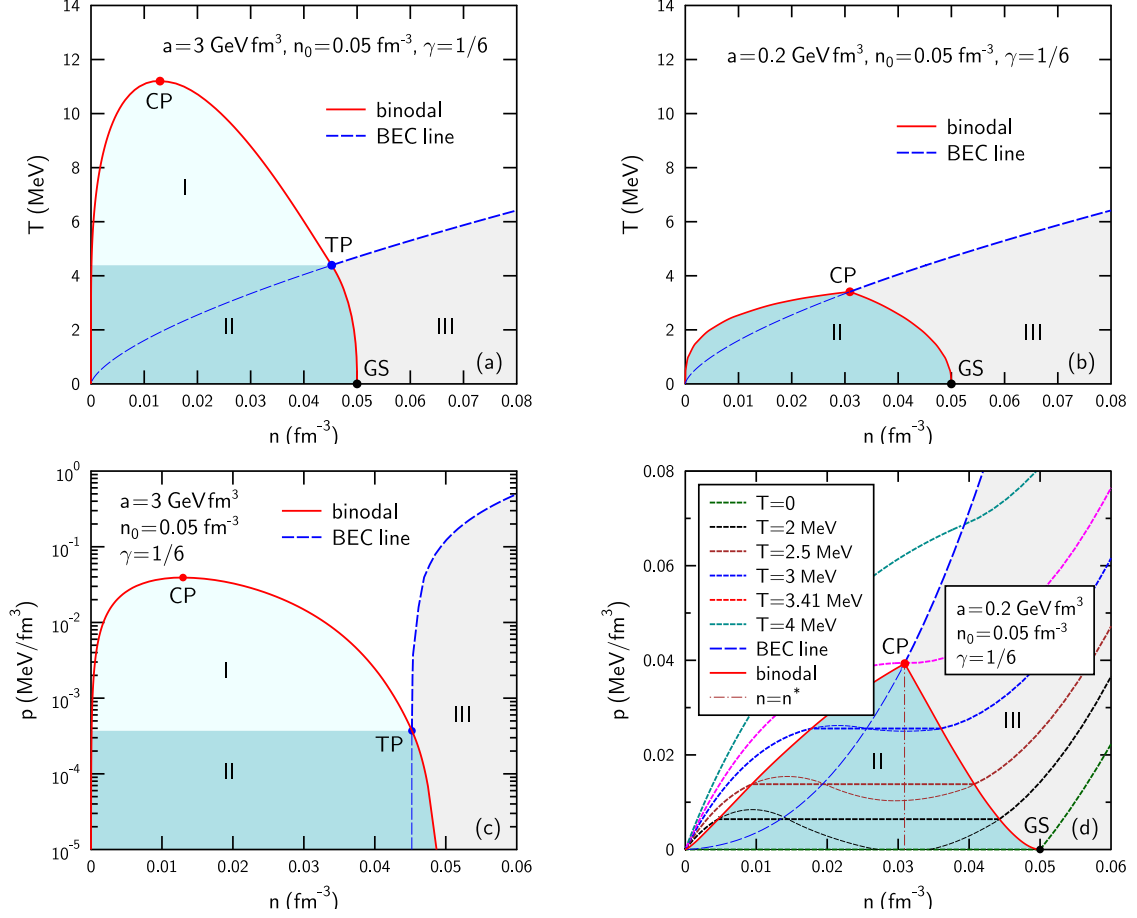


FIG. 3: Solid lines in all panels show the boundary of the mixed phase, and dashed curves correspond to the BEC lines. (a): The phase diagram of the  $\alpha$ -matter in the  $(n, T)$  plane for the same model parameters as in Figs. 1 and 2. The region I corresponds to the mixed phase with  $n_{bc} = 0$ , the region II to the mixed phase with nonzero  $n_{bc}$  in the liquid component, and the region III to the pure liquid phase with  $n_{bc} > 0$ . (b): The same as (a) but for  $a = 0.2 \text{ GeV fm}^3$ . Here the CP and TP coincide, and the region I is absent (see text for details). (c): The phase diagram in the  $(n, p)$  plane for the same parameters as in panel (a). The logarithmic scale is used to show the region II. (d): The same as (c) but for  $a = 0.2 \text{ GeV fm}^3$  (see text for details).

the CP has a fixed position

$$T_c = T_{\text{BEC}}(n^*), \quad n_c = n^* \quad (a \leq a_s). \quad (18)$$

In Figs. 3 (b) and (d) we present the results for  $\gamma = 1/6$  and  $n_0 = 0.05 \text{ fm}^{-3}$  (these parameters are the same as in panels (a) and (c)), but choose  $a = 0.2 \text{ GeV fm}^3$ . In this case,  $a$  is smaller than the value  $a_s \simeq 358 \text{ MeV fm}^3$  obtained from (17) and, therefore, the CP

position is determined by Eq. (18). Several pressure isotherms are shown in Fig. 3 (d). Thin lines represent metastable and unstable parts of the isotherms. The position of the RHS spinodal is shown by the vertical dash-dotted line. One can see a 'kink' between the left- and right-hand side binodals at the CP.

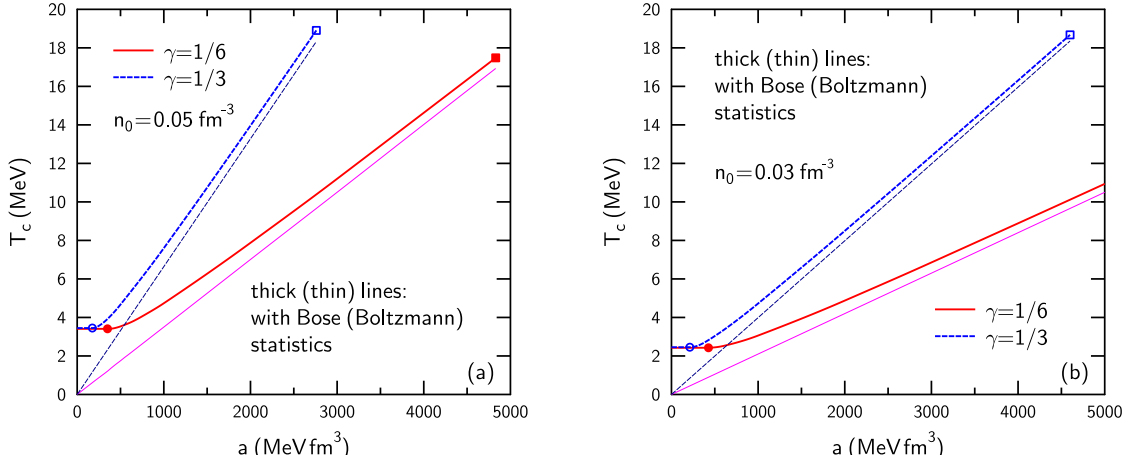


FIG. 4: Critical temperature of  $\alpha$ -matter as a function of coupling constant  $a$  for  $\gamma = 1/6$  (solid curves) and  $1/3$  (dashed lines). Thick and thin lines correspond, respectively, to quantum-statistical and Boltzmann calculations. The dots show the onset of the saturation regime (see the text). The squares give maximum possible values of the parameter  $a$ . (a):  $n_0 = 0.05 \text{ fm}^{-3}$  and (b):  $n_0 = 0.03 \text{ fm}^{-3}$ .

TABLE II: Characteristics of the CP in the saturation regime.

$n_0 \text{ (fm}^{-3}\text{)}$	$\gamma$	$a_s \text{ (MeV fm}^3\text{)}$	$n^* \text{ (fm}^{-3}\text{)}$	$T_{\text{BEC}}(n^*) \text{ (MeV)}$
0.05	1/6	358	0.0310	3.41
0.05	1/3	178	0.0315	3.45
0.03	1/6	427	0.0186	2.43
0.03	1/3	212	0.0189	2.46

The dependence of  $T_c$  on the parameters  $a$ ,  $\gamma$ ,  $n_0$  is illustrated in Fig. 4 and in Table II. The upper limits for  $a$  in Fig. 4 are taken from the requirement that the binding energy per baryon in the ground state of  $\alpha$ -matter is smaller than 16 MeV, i.e., the estimated binding energy of homogeneous isospin-symmetric nucleon matter at  $T = 0$ . As seen from Fig. 4

the Boltzmann approximation fails at small values of  $a$ . Therefore, the saturation of  $T_c$  at  $a \rightarrow 0$  is a pure quantum effect, a consequence of the Bose statistics. Due to the BEC effects, the system exhibits the LGPT with the CP given by Eq. (18) even for an infinitely small interaction coupling  $a$ . This happens due to the special form (7) of the interaction potential  $U(n)$ , but may occur also in other situations.

Some properties of the CP at  $a \leq a_s$  are similar to those at  $a > a_s$ : 1) it is the end point of the LGPT; 2)  $(\partial p / \partial n)_T = 0$  and  $\omega = \infty$  at  $T = T_c$  and  $n = n_c$ . However, there are some essential differences: at  $a > a_s$ , one has in addition  $(\partial^2 p / \partial n^2)_T = 0$ . Hence, the behavior of thermodynamical functions in the vicinity of the CP is governed by the critical indices which belong to the universality class of the van der Waals model (the so-called mean-field theory). At  $a \leq a_s$ , the second derivative  $(\partial^2 p / \partial n^2)_T$  has a discontinuity at the CP. In this case the standard concept of the critical indices should be reconsidered. Note that in this case the left- and right-hand side binodals are essentially different in the vicinity of the CP: the left-hand side binodal consists of gas states with  $n_{bc} = 0$ , whereas the states on right one correspond to the liquid with a nonzero Bose-condensate.

#### IV. CONCLUDING REMARKS

We have analyzed the phase diagram of pure  $\alpha$ -matter within a simple model using a density-dependent mean-field interaction. This model does not only predict the liquid-gas mixed phase at low temperatures, but simultaneously it describes the Bose-Einstein condensation. The interplay between these two phenomena shows new important effects.

The end point of the LGPT is located on the BEC line at small values of the interaction coupling, where the standard description of the critical point is not applicable. This behavior may also occur in other multiparticle systems. In particular, we expect to find similar effect in atomic Bose systems.

Pure  $\alpha$ -matter at nonzero temperatures is an idealization which does not respect the chemically equilibrium conditions. A more realistic approach should include also nucleons and nucleon clusters like  $d, t, {}^3\text{He}$ . The equilibrium mixture of nucleons and light nuclei are important for heavy-ion collisions and astrophysical applications. This topic will be addressed in future studies.

## Acknowledgments

The authors thank D. V. Anchishkin for useful discussions. A.M. is thankful for the support from the Eurasia grant No. CPEA-LT-2016/10094. The work of M.I.G. is supported by the Goal-Oriented Program of the National Academy of Sciences of Ukraine, by the European Organization for Nuclear Research (CERN), Grant CO-1-3-2016, and by the Program of Fundamental Research of the Department of Physics and Astronomy of National Academy of Sciences of Ukraine. V.V. appreciates the support from HGS-HIRe for FAIR.

---

- [1] S. N. Bose, Z. Phys. 26, **178** (1924).
- [2] A. Einstein, Sitz. Ber. Preuss. Akad. Wiss. (Berlin) **1**, 3 (1925).
- [3] M. H. Anderson, et al., Science **269**, 198 (1995).
- [4] K. B. Davis, et al., Phys. Rev. Lett. **75**, 3969 (1995).
- [5] C. J. Pethick and H. Smith, *Bose-Einstein Condensation in Dilute Gases* (Cambridge University Press, 2002).
- [6] L. Pitaevskii, and S. Stringari, *Bose-Einstein Condensation* (Clarendon, Oxford, 2003).
- [7] C. Chin, R. Grimm, P. Julienne, and E. Tiesinga, Rev. Mod. Phys. **82**, 1225 (2010).
- [8] L. D. Landau and E. M. Lifshitz, *Statistical Physics* (Pergamon, Oxford, 1975).
- [9] W. Greiner, L. Neise, and H. Stöcker, *Thermodynamics and Statistical Mechanics* (Springer, 1997).
- [10] W. A. Küpper, G. Wegmann, and E. R. Hilf, Ann. Phys. (N.Y.) **88**, 454 (1974).
- [11] H. Jaqaman, A. Z. Mekjian, and L. Zamick, Phys. Rev. C **27**, 2782 (1983).
- [12] H. Buchenau, E. L. Knuth, J. Northby, J. P. Toennies, C. Winkler, J. Chem. Phys. **92**, 6875 (1990).
- [13] E. M. Lifshitz, L. P. Pitaevskii, *Statistical Physics, Part 2: Theory of the Condensed State* (Pergamon Press, Oxford, 1980).
- [14] J. W. Clark, T.-P. Wang, Ann. Phys. **40**, 127 (1966).
- [15] D. M. Brink, J. J. Castro, Nucl. Phys. A **216**, 109 (1973).
- [16] W. von Oertzen, M. Freer, Y. Kanada-En'yo, Phys. Rept. **432**, 43 (2006).
- [17] *Clusters in Nuclei, Vol. 2*, Lect. Notes Phys. vol. 848, ed. by C. Beck (Springer-Verlag,

- Berlin, 2012).
- [18] P. Schuck, Y. Funaki, H. Horiuchi, G. Röpke, A. Tohsaki, and T. Yamada, Phys. Scripta **91**, 123001 (2016).
  - [19] G. Röpke, A. Schnell, P. Schuck, P. Nozières, Phys. Rev. Lett. **80**, 3177 (1998).
  - [20] J. P. Bondorf, A. S. Botvina, A. S. Iljinov, I. N. Mishustin, K. Sneppen, Phys. Rept. **257**, 133 (1995).
  - [21] P. Marini *et al.* (INDRA Collaboration), Phys. Lett. B **756**, 194 (2016).
  - [22] B. Borderie *et al.*, Phys. Lett. B **755**, 475 (2016).
  - [23] S. Typel, G. Röpke, T. Klähm, D. Blaschke, and H. Wolter, Phys. Rev. C **81**, 015803 (2010).
  - [24] A. S. Botvina and I. N. Mishustin, Nucl. Phys. A **843** 98 (2010).
  - [25] J. M. Lattimer, F. D. Swesty, Nucl. Phys. A **535**, 331 (1991).
  - [26] N. Buyukcizmeci, A. S. Botvina, I. N. Mishustin, Astrophys. J. **789**, 33 (2014).
  - [27] C. J. Horowitz, A. Schwenk, Nucl. Phys. A **776**, 55 (2006).
  - [28] Ş. Mişicu, I. N. Mishustin, and W. Greiner, Mod. Phys. Lett. A **32**, 1750010 (2017).
  - [29] A. Sedrakian, H. Müther, P. Schuck, Nucl. Phys. A **786**, 97 (2006).
  - [30] J. Hofmann, H. Stöcker, U. Heinz, W. Scheid, W. Greiner, Phys. Rev. Lett. **36**, 88 (1976).
  - [31] V. M. Galitskii and I. N. Mishustin, Phys. Lett. **72B**, 285 (1978).
  - [32] I. N. Mishustin, V. N. Russkikh, L. M. Satarov, Sov. J. Nucl. Phys. **54**, 260 (1991).
  - [33] L. M. Satarov, M. N. Dmitriev, I. N. Mishustin, Phys. At. Nucl. **72**, 1390 (2009).
  - [34] M. Bender, P.-H. Heenen, and P.-G. Reinhard, Rev. Mod. Phys. **75**, 121 (2003).
  - [35] J.R. Stone, P.-G. Reinhard, Prog. Part. Nucl. Phys. **58**, 587 (2007).
  - [36] V. Vovchenko, D. V. Anchishkin, M. I. Gorenstein, and R. V. Poberezhnyuk, Phys. Rev. C **92**, 054901 (2015).
  - [37] V. Vovchenko, arXiv: 1701.06524 [nucl-th].
  - [38] V. V. Begun and M. I. Gorenstein, Phys. Lett. B **653**, 190 (2007); Phys. Rev. C **77**, 064903 (2008).